

Effects of thermal aging on Fe ion-irradiated Fe–0.6%Cu alloy investigated by positron annihilation

Yuan-Chao Hu^{1,2} · Xing-Zhong Cao¹ · Peng Zhang¹ · Hidetsugu Tsuchida³ · Qiu Xu⁴ · Shuo-Xue Jin¹ · Er-Yang Lu¹ · Yu-Xiao Li² · Run-Sheng Yu¹ · Bao-Yi Wang¹ · Long Wei¹

Received: 20 January 2016/Revised: 28 April 2016/Accepted: 21 May 2016/Published online: 24 December 2016
© Shanghai Institute of Applied Physics, Chinese Academy of Sciences, Chinese Nuclear Society, Science Press China and Springer Science+Business Media Singapore 2016

Abstract Thermal aging effects on surface of 2.5 MeV Fe ion-irradiated Fe–0.6%Cu alloy were investigated using positron annihilation techniques. The samples were irradiated at 573 K to a dose of 0.1 dpa. Their thermal aging was performed at 573 K for 5, 50 and 100 h. From the results of Doppler broadening measurement, an obvious trough could be seen in near-surface region from the *S* parameters and inflection point form at *S–W* curves. This indicates changes in the annihilation mechanism of positrons in surface region after thermal aging. Coincident Doppler broadening indicates that the density of Cu precipitates in the thermal aged samples decreased, due to recovery of the vacancies.

Keywords Fe–Cu alloy · Positron annihilation · Irradiation · Thermal aging

1 Introduction

It is well known that Cu precipitates in iron-based alloys play an important role in steel embrittlement of reactor pressure vessel (RPV) [1–6]. The interaction mechanism between Cu precipitates and microdefects during deformation, irradiation, or aging has attracted interests in RPV steels studied in the past decades [5, 7–11]. Especially, the Cu precipitate would cause hardening/embrittlement in RPV steels, which is a serious degradation in operation of nuclear reactors [4–8, 12, 13].

In experiments of self-ion (heavy ion) irradiation in the RPV steels, model Fe–Cu alloys could be a proper system to study Cu precipitates [14]. In our previous work of Cu-rich precipitates due to 2.5 MeV Fe ion irradiation, it was found that Cu precipitates interacted with defects in Fe–Cu alloys irradiated at 573 K by slow positron beam [15]. As the RPV steel under long-term aging and reactor operation temperature of ~573 K, it is important to investigate effects of the Cu-rich precipitates induced by thermal aging in RPV steels, and to understand the embrittlement caused by the Cu-rich precipitates [16].

In the present paper, the Fe–0.6%Cu is heated under 10^{-4} Pa vacuum to 573 K for 5, 50, and 100 h. For characterizing the thermal aging effect on the surface region, techniques of the Doppler broadening spectroscopy (DBS) and coincident Doppler broadening (CDB), based on slow positron beam, are used.

This work was supported by the National Natural Science Foundation of China (Nos. 91026006, 91226103, 11475193, 11475197, 11575205 and 11505192) and Beijing Natural Science Foundation (No. 1164017).

✉ Xing-Zhong Cao
caozh@ihep.ac.cn

¹ Institute of High Energy Physics, Chinese Academy of Sciences, Beijing 100049, China

² College of Physical Engineering, Zhengzhou University, Zhengzhou 450001, China

³ Quantum Science and Engineering Center, Kyoto University, Uji 6110011, Japan

⁴ Research Reactor Institute, Kyoto University, Osaka 5900494, Japan

2 Experimental procedure

Fe–0.6%Cu alloy was formed by melting Fe (99.99% purity) and Cu (99.999% purity) in vacuum by a high-frequency induction furnace. The specimens were kept at 1173 K for 4 h in high-purity hydrogen gas, followed by quenching into iced water. The specimens, sized at 8 mm × 8 mm × 0.2 mm, were irradiated with 2.5 MeV Fe ions to 0.1 dpa (displacement per atom) at 573 K in a tandem pelletron accelerator (model: 6SDH-2), in the Quantum Science and Engineering Center, Kyoto University. The thermal aging was conducted at 573 K under 10^{-4} Pa vacuum for 5, 50, and 100 h, respectively.

Positron annihilation technique (PAT), with an energy-variable slow positron beam facility, was performed at Institute of High Energy Physics. The slow positron beams were from a 50 mCi (2005) ^{22}Na source, moderated by tungsten. Beam energy was 0.18–25 keV. The mean depth of annihilated positrons was calculated by the empirical equation of $z(E) = 40E^{1.6}/\rho$, where z is expressed in nanometer, ρ is the material density in g/m^3 , and E is the incident positron energy in keV. DBS was used to characterize the surface defects distribution. A high-purity Germanium detector (HPGe) was used to record the 511 keV peak of positron annihilation.

Normally, S and W parameters are used to evaluate annihilation characteristics in the DBS. S parameter is defined as the ratio of γ -ray counts in central part of the 511 keV peak (510.20–511.80 keV) to the total counts of entire spectrum (503.34–518.66 keV). And W parameter is defined as the ratio of counts in the wing areas (514.83–518.66 and 503.34–507.17 keV) to the total counts of entire spectrum. The information of annihilation mechanism of positrons with low/high-momentum electrons in materials can be reflected by the S/W parameters, respectively. CDB with two HPGe detectors determines the high-momentum distribution of electrons annihilated with positrons such as the 3d Cu electrons. It can measure the impurity atoms definitely around the annihilation sites at interested depth by decreasing the background of high-momentum contributions.

3 Results and discussion

3.1 Irradiation effects

Figure 1a shows the SEM image of the Fe–0.6%Cu alloy irradiated to 0.1 dpa by 2.5 MeV Fe ions at 573 K. The crystalline structure formed many tiny clusters on the surface, aggregating at the grain boundary especially. It was reported in Refs. [9, 15] that Cu atoms migrated with diffusion of vacancies and aggregated at the grain

boundary [9, 15]. Figure 1b shows that the S parameter decreased with increasing positron energy from 0.18 to 20 keV, corresponding to the depth of ~ 0.65 μm . This depth is almost close to the irradiated vacancy peak area induced by 2.5 MeV Fe ions, according to the simulation results using the TRIM code. This indicates that, comparing to the non-irradiated sample, the 0.1 dpa Fe ion irradiation increases S parameters, except the near surface in the positron energy range of 1–5 keV. At the near surface of thinner than 0.1 μm , the decrease in S parameters for the irradiated sample can be attributed to the Cu precipitates crystalline on the grain boundary, which could change the diffusion length of positron.

3.2 Thermal aging effects

The irradiated samples were thermal aged in high vacuum at 573 K for different hours. Doppler broadening analysis of slow positron beam was carried out with the samples. Figure 2 shows the S – E and W – E curves, and S – W slots. In Fig. 2a, over positron energy of 10.0 keV, the decreasing S parameters of the sample thermal aged for 50 h approached the results of the non-irradiated sample. This indicates that the vacancy defects, as main defects formed by Fe ions irradiation, had migrated and almost recovered after the longtime thermal aging at 573 K [16]. Also, the increasing W parameters in Fig. 2b indicate the migration and aggregating of Cu precipitates along with the thermal dynamic of vacancies defects, because of the irradiation of Fe ions. This is also confirmed by the S – W plots in Fig. 2c, in which the slope increases with the thermal aging time as marked by the arrows. It can be assumed that the annihilation mechanism of positrons is changed.

The annihilation of positrons below 5 keV is attributed to the defects near the surface. The thermal dynamics of defects and Cu precipitates is complicated near the surface, as shown by the Doppler broadening results of slow positron beam. In 50 and 100 h thermal aging, the S parameters show a lower trough near 1.5 keV. This phenomenon may be attributed to two factors. One is the backscattered positrons. When positrons incident on the surface of materials, most positron reflected elastically from the surface annihilates with electron outside the materials. The coefficient for the backscattered positrons increases with the atomic numbers (Z) of the metal target [17, 18]. And it seems that, in Fig. 2a, the longer is the thermal aging, the smaller is the averaged atomic number of the specimen. Another factor is the recovery of some microvoids by dissociating their vacancies, hence the reduced probability of positron annihilation. W parameters of the specimen thermal aged for longer hours are almost fitted with non-irradiated specimen below 2 keV. It could be assumed that

Fig. 1 SEM image of the Fe–0.6%Cu irradiated by 2.5 MeV Fe ions (a) and *S* parameters of slow positron beam and vacancy distribution simulated by TRIM (b)

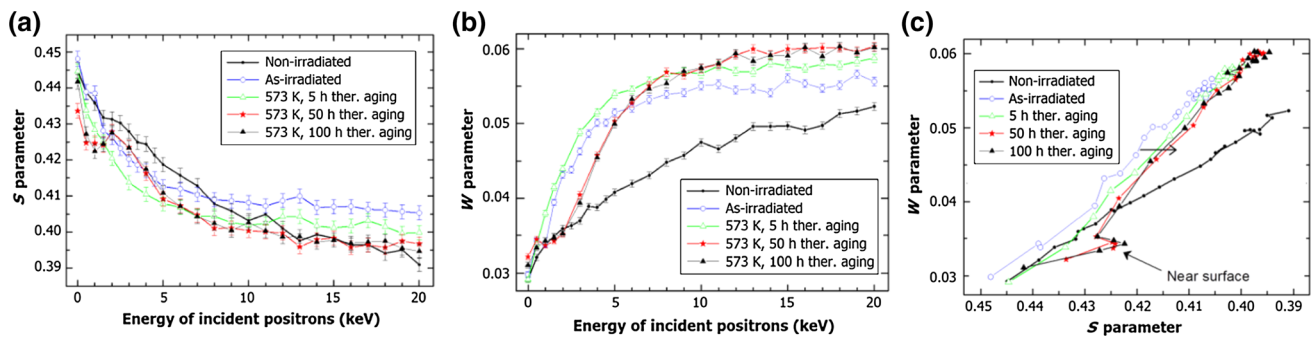
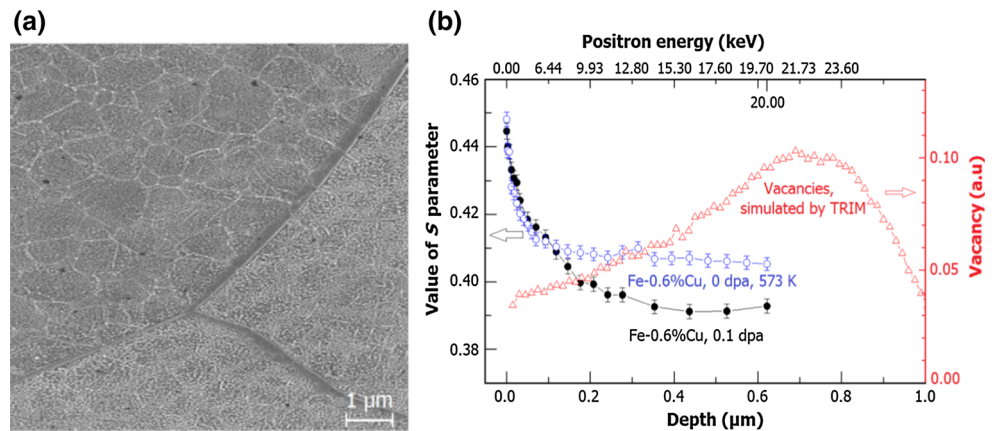


Fig. 2 *S* and *W* parameters (a, b) as function of positron energy and the *S*–*W* diagram (c), for Fe–0.6%Cu samples treated differently

the *W* parameter is not contributed from annihilation with Cu precipitates. In the *S*–*W* diagram, the appearance of an inflection point can confirm that the annihilation mechanism of positrons is changed at near surface. However, for the irradiated sample thermal aged for 5 h, the *S* and *W* parameters change in the same tendency, indicating that the annihilation mechanism is similar. For the samples of longer thermal aging hours, the slope of the *S*–*W* plots in subsurface area is the same as the sample of 5-h thermal aging, while in near-surface area it is close to the non-irradiated. This indicates that in longtime thermal aging, the annihilation mechanism of positrons is similar to the substrate in near-surface area.

To distinguish the annihilation mechanism of positrons and characterize the precipitates of Cu atoms in near surface, CDB experiments, with an as-irradiated sample and the sample just after 50-h thermal aging, along with the pure Fe and Cu samples, and the control, were performed at positron energy of 1.5 keV, corresponding to the inflection point at *S*–*W* diagram. The results of ratio to pure Fe are shown in Fig. 3. At high-momentum region, the information of annihilation mechanism of positrons with the core of electron is provided. For the core electrons, the 3d electron shell of Fe atom differs from that of Cu atom, so the broad peak around $25 \times 10^{-3} m_0c$ characteristic of Cu 3d electrons is clearly observed for pure Cu specimen. The

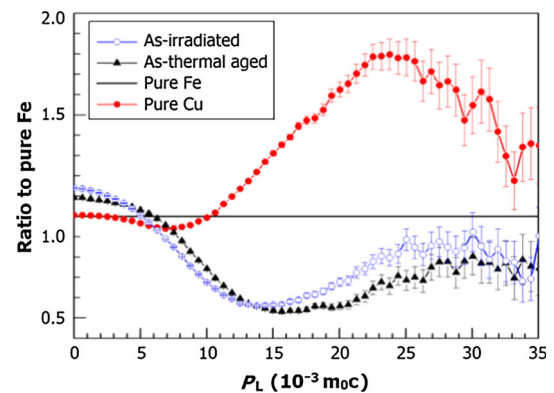


Fig. 3 CDB spectrums for irradiated and thermal aged Fe–0.6%Cu alloy with 1.5 keV positron beam energy

increase of counts in the low-momentum region and the decrease in the high-momentum region correspond to the inflection point at *S*–*W* diagram. If the Cu precipitates in the specimens, the Cu peak will appear in the CDB spectrum. In Fig. 3, some unobvious Cu peaks can be seen in both the as-irradiated and as-thermal aged curves. It seems that the number of Cu atoms is less, in accord with the *W* parameters in Fig. 2b. In Fig. 3, the ratios of the two irradiated samples are higher than 1 in low-momentum region ($<5 \times 10^{-3} m_0c$), showing that the positrons annihilated mainly with low-momentum electrons, and more

positrons were trapped in the irradiation-induced microvoids, vacancies, and dislocation loops. The Cu CDB signal can be observed only when the positrons are localized around the Cu atoms in the dilute alloys: trapped at vacancy-type defects bound to Cu atoms or confined in Cu precipitates [5]. In low-momentum area ($<5 \times 10^{-3} m_0c$), the spectrum of thermal aged is lower than irradiated, because the irradiated specimen had more defects and part of the microvoids recovered in the thermal aging. In high-momentum region, the ratios of the thermal aged are lower than 1. A possible interpretation is that the density of Cu precipitates decreases due to aggregation of the small precipitates and positrons annihilate in the matrix [19]. As the precipitates grow larger, they undergo transformations such as bcc to 9R structure [20], corresponding to the change of S - W curves. All these indicate that density of the irradiation-induced Cu precipitates decreases in the near surface by thermal aging for 50 h.

4 Conclusion

The irradiation damage by 2.5 MeV Fe ions and long-time thermal aging effect for Fe–0.6%Cu alloy are investigated by PAT. S parameters and S - W diagram of Doppler broadening spectroscopy indicate that the annihilation mechanism of positrons changes in near surface. It can also be concluded from W parameters and CDB spectra that the density of Cu precipitates decreased after longtime thermal aging (50 and 100 h). In the present Fe–Cu system of irradiation-induced precipitation, the longtime thermal aging makes the Cu aggregations and part of the vacancy-type defects recover near the surface.

References

1. F. Soisson, C. Fu, Cu-precipitation kinetics in α -Fe from atomistic simulations: vacancy-trapping effects and Cu-cluster mobility. *Phys. Rev. B* **76**, 214102 (2007). doi:10.1103/PhysRevB.76.214102
2. S.I. Golubov, Y.N. Osesky, A. Serra et al., The evolution of copper precipitates in binary Fe–Cu alloys during ageing and irradiation. *J. Nucl. Mater.* **226**, 252–255 (1995). doi:10.1016/0022-3115(95)00088-7
3. G.J. Ackland, D.J. Bacon, A.F. Calder et al., Computer simulation of point defect properties in dilute Fe–Cu alloy using a many-body interatomic potential. *Philos. Mag. A* **75**, 713–732 (1997). doi:10.1080/01418619708207198
4. M. Lambrecht, A. Almazouzi, Positron annihilation study of neutron irradiated model alloys and of a reactor pressure vessel steel. *J. Nucl. Mater.* **385**, 334–338 (2009). doi:10.1016/j.jnucmat.2008.12.020
5. Y. Nagai, Z. Tang, M. Hasegawa et al., Irradiation-induced Cu aggregations in Fe: an origin of embrittlement of reactor pressure vessel steels. *Phys. Rev. B* **63**, 134110 (2001). doi:10.1103/PhysRevB.63.134110
6. J.Z. Liu, A. Walle, G.F. Ghosh et al., Structure, energetics, and mechanical stability of Fe–Cu bcc alloys from first-principles calculations. *Phys. Rev. B* **72**, 144109 (2005). doi:10.1103/PhysRevB.72.144109
7. D. Molnar, P. Binkele, S. Hocker et al., Atomistic multiscale simulations on the anisotropic tensile behavior of copper-alloyed alpha-iron at different states of thermal ageing. *Philos. Mag.* **92**, 586–607 (2012). doi:10.1080/14786435.2011.630690
8. B. Minov, M. Lambrecht, D. Terentyev et al., Structure of nanoscale copper precipitates in neutron-irradiated Fe–Cu–C alloys. *Phys. Rev. B* **85**, 024202 (2012). doi:10.1103/PhysRevB.85.024202
9. G.R. Odette, On the dominant mechanism of irradiation embrittlement of reactor pressure vessel steels. *Scr. Metall.* **17**, 1183 (1983). doi:10.1016/0036-9748(83)90280-6
10. T. Ishizaki, T. Yoshiie, K. Sato et al., Precipitation of Cu in Fe–Cu alloys by high-speed deformation. *Mater. Sci. Eng. A* **350**, 102–107 (2003). doi:10.1016/S0921-5093(02)00706-2
11. Y. Nagai, K. Takadate, Z. Tang et al., Positron annihilation study of vacancy-solute complex evolution in Fe-based alloys. *Phys. Rev. B* **67**, 224202 (2003). doi:10.1103/PhysRevB.67.224202
12. R.G. Carter, N. Sonedab, K. Dohib et al., Microstructural characterization of irradiation-induced Cu-enriched clusters in reactor pressure vessel steels. *J. Nucl. Mater.* **298**, 211–224 (2001). doi:10.1016/S0022-3115(01)00659-6
13. Z. Chen, N. Kioussis, N. Ghoniem, Influence of nanoscale Cu precipitates in α -Fe on dislocation core structure and strengthening. *Phys. Rev. B* **80**, 184104 (2009). doi:10.1103/PhysRevB.80.184104
14. K. Morita, S. Ishino, T. Tobita et al., Use of high energy ions for the mechanistic study of irradiation embrittlement in pressure vessel steels using Fe–Cu model alloys. *J. Nucl. Mater.* **304**, 153–160 (2002). doi:10.1016/S0022-3115(02)00877-2
15. X.Z. Cao, P. Zhang, Q. Xu et al., Cu precipitates in Fe ion irradiated Fe–Cu alloys studied using positron techniques. *J. Phys. C* **443**, 012017 (2013). doi:10.1088/1742-6596/443/1/012017
16. H.B. Wu, X.Z. Cao, G.D. Cheng, et al., Effects of copper precipitates on microdefects in deformed Fe–1.5 wt%Cu alloy. *Phys. Status. Solidi. A* **210**, 1758–1761 (2013). doi:10.1002/pssa.201228849
17. J.A. Baker, P.G. Coleman, Measurement of coefficients for the back-scattering of 0.5–30 keV positrons from metallic surfaces. *J. Phys. C* **21**, L875–L880 (1988). doi:10.1088/0022-3719/21/23/003
18. A.P. Knights, P.G. Coleman, The observation of structure in the dependence of the 1 keV positron backscattering coefficient on target atomic number. *J. Phys.: C Matter.* **7**, 3485–3492 (1995). doi:10.1088/0953-8984/7/18/012
19. Y. Nagai, M. Hasegawa, Z. Tang, et al., Positron confinement in ultrafine embedded particles: quantum-dot-like state in an Fe–Cu alloy. *Phys. Rev. B* **61**, 6574 (1999). doi:10.1103/PhysRevB.61.6574
20. Q.L. Wang, J.Z. Zhao, A model describing the microstructure evolution in Fe–Cu alloys during thermal aging. *Mater. Sci. Eng. A* **528**, 268–272 (2010). doi:10.1016/j.msea.2010.09.012